ELSEVIER

15 June 1999

Optics Communications 164 (1999) 233–245

OPTICS COMMUNICATIONS

www.elsevier.com/locate/optcom

Full length article

Fast algorithms for free-space diffraction patterns calculation

David Mas [a,1], Javier Garcia [b], Carlos Ferreira [b], Luis M. Bernardo [c], Francisco Marinho [c]

[a] *Dept. Interuniversitari d'Òptica,Universitat d'Alacant, P.O. Box 99, E-03080 Alacant, Spain*
[b] *Dept. Interuniversitari d'Òptica, Universitat de València, C / Doctor Moliner 50, 46100 Burjassot Valencia, Spain*
[c] *CETO / Departamento de Física, Faculdade de Ciencias, Universidade do Porto, R. do Campo Alegre, 687, 4150 Porto, Portugal*

Received 3 February 1999; received in revised form 15 April 1999; accepted 20 April 1999

Abstract

Here we present a fast algorithm for Fresnel integral calculation. Some fast algorithms using the fast Fourier transform are analysed and their performance has been checked. These methods are of easy implementation, but are only valid for a specific range of distances. Fast algorithms based on the Fractional Fourier transform allow accurate evaluation of the Fresnel integral from object to Fraunhofer domain in a single step.

Keywords: Fresnel integral calculation; Discrete Fourier transform; Fast Fourier transform; Fractional Fourier transform

1. Introduction

Fresnel diffraction is a classical topic in wave optics since this formalism describes beam propagation between object and Fourier domain. Although most practical problems may be treated in those two domains, in many cases it is interesting a more general Fresnel diffraction treatment. Unfortunately, accurate evaluation of diffraction patterns is not an easy task. Among the different diffraction domains, only two admit a clear analytic or numerical treatment: one of them is the object domain, which corresponds to the trivial case. The other one is the Fraunhofer domain, that can be evaluated by means of the Fourier Transform. Under some general assumptions (see Ref. [1], for instance), the Fourier transform can be numerically evaluated through the Discrete Fourier Transform (DFT). Efficient implementation of the DFT can be performed through the Fast Fourier Transform (FFT) algorithm [2].

For the most general case of Fresnel patterns calculation, the solution is not so clear. Analytical calculation of the Fresnel integral is not always possible, and, in any case, this calculation does not always ensure an accurate sampling of the output. Furthermore, calculation of diffraction integrals is usually very inefficient (time consuming) and thus direct evaluation methods are not suitable for intensive calculation of Fresnel patterns.

The Fresnel pattern produced by an object u_0 at a distance z when it is illuminated by a monochro-

[1] E-mail: david.mas@ua.es

0030-4018/99/$ - see front matter
PII: S0030-4018(99)00201-1

matic plane wave whose wavelength is λ can be expressed as:

$$u_z(x_z) = u_0(x_z) * \exp\left(i\frac{\pi}{\lambda z}x_z^2\right) = \exp\left(i\frac{\pi}{\lambda z}x_z^2\right)\int_{-\infty}^{+\infty}\left[u_0(x_0)\exp\left(i\frac{\pi}{\lambda z}x_0^2\right)\right] \times \exp\left(-i\frac{2\pi}{\lambda z}x_z x_0\right)\mathrm{d}x_0 \quad (1)$$

where constant factors have been dropped. In this expression, and in the remainder of the paper, we will use 1-D formulation. Extension to 2-D is straightforward.

Let us consider the input object $u_0(x)$ being of finite extent Δx_0 and let us assume that its frequency content is negligible outside a band of extension $\Delta\nu_0$. This last assumption implies that the frequency extent of the output signal $\Delta\nu_z$ remains invariant while the pattern propagates. This can be checked by taking the Fourier transform of Eq. (1):

$$\mathcal{F}[u_z] = \tilde{u}_z = \tilde{u}_0 \times \exp(-i\pi\lambda z\nu^2) \approx \mathrm{rect}\left(\frac{\nu}{\Delta\nu_0}\right) \times \tilde{u}_0 \times \exp(-i\pi\lambda z\nu^2) \quad (2)$$

with ν being the variable in the frequency domain. From Nyquist theorem [3], good sampling of a pattern requires that the sampling rate, δx_z fulfills:

$$\delta x_z \le \frac{1}{\Delta\nu_{z_{\max}}} \equiv \frac{1}{\Delta\nu_0} \quad (3)$$

and thus, it will remain constant independently of the considered distance. On the other hand, note that the physical extension of the diffracted pattern, Δx_z enlarges with the distance:

$$\Delta x_z = \Delta x_0 + \lambda z\Delta\nu_0 \quad (4)$$

Therefore, accurate evaluation of a propagated pattern requires an increasing number of sampling points N at the output plane. It is worth to point that this limitation is imposed by the integral itself and not by the evaluation method.

At this point we have three different ways of evaluating Fresnel patterns:

- Increasing N with z, and thus, maintaining constant δx_z. This option is not operative for $z \to \infty$.
- Maintaining δx_z and N as constants. Thus, for $z \to \infty$, the relative portion of the output plane that is being sampled goes to zero.
- Increasing the sampling period δx_z with the distance while the number of samples in each pattern will remain the same.

Dealing with specific digital calculation methods, several numerical techniques have been proposed for diffraction integral computations [4–7]. Unfortunately, the techniques there proposed do not lead to easy algorithms of immediate and simple analysis and implementation.

Fourier transform-based methods [8,9] provide facile implementation and understanding since DFT algorithm is of wide-use in signal processing tasks. The main drawback of these methods is the requirement of two different algorithms for Fresnel pattern calculation: one for near-field patterns and another for the far-field case.

An alternative formalism for dealing with domains between object plane and Fourier domain is the fractional Fourier transform (FRT) [10–12]. Methods for calculating the FRT through the fast Fourier transform algorithm are also available [8,13]. These methods allow the calculation of FRT patterns for all the range of orders between object an Fourier domain in one single step, by using one simple algorithm.

The relationship between Fresnel diffraction patterns and FRT patterns has been shown in many papers by different methods [14–19]. This relation may be exploited here to calculate the Fresnel diffraction patterns through a fast FRT algorithm.

The motivation of this paper is to analyze FFT-based algorithms for Fresnel integral calculation. Taking into account the inherent limitations of the Fresnel integral calculation, direct methods [8,9] will be analyzed and their restrictions will be clearly stated. These direct methods do not cover all the range of propagation distances from zero to infinite. We will show here that FRT-based methods overcome this problem and, to our knowledge, permit the calculation of Fresnel patterns up to theoretical limits. Furthermore, the final algorithm that will be presented here is of easy implementation and understanding, and will allow the calculation of a Fresnel pattern in FFT time.

In Section 2 FFT-based methods presented in Refs. [8,9] for diffraction patterns calculation will be

reviewed. In Section 3, FRT based for Fresnel calculation algorithms will be introduced, and their performance will be studied in Section 4. Some numerical simulation, in Section 5, will show the performance of the different methods here discussed. Finally, the main conclusions will be outlined in Section 6.

2. FFT-based algorithms for Fresnel diffraction calculation

From Eq. (1) it is clear that Fresnel diffraction integral can be interpreted as the Fourier transform of the product of the input signal and a quadratic phase factor. The whole result is also multiplied by a quadratic phase factor.

Expression (1) can be calculated by means of the DFT, just by proper sampling of the integral. Let us consider Δx_0 and Δx_z the sampling extensions at object and Fresnel domain, and N the number of samples in both domains. Therefore, by imposing the following relation:

$$\Delta x_0 \Delta x_z = \lambda z N \tag{5}$$

the sampled version of Eq. (1) results into:

$$(u_z)_{m'} = \exp\left(i\pi \frac{\lambda z}{\Delta x_0^2} m'^2 \right) \times \mathrm{DFT}\left[u_0\left(\frac{m \Delta x_0}{N} \right) \exp\left(i\pi \frac{\Delta x_0^2}{\lambda z N^2} m^2 \right) \right] \tag{6}$$

where

$$x_0 = m\delta x_0, \quad x_z = m\delta x_z \tag{7}$$

$\delta x_0 = \Delta x_0/N$ and $\delta x_z = \Delta x_z/N$ are the sampling periods in the object and Fresnel domain, and m and m' are integers [8].

The expression written in Eq. (6) will provide a good evaluation of the Fresnel pattern if the Nyquist sampling condition is fulfilled [3]. Assuming that the object $u_0(x_0)$ has frequencies smaller than those in the quadratic phase factors, the main problem when calculating Eq. (6) comes from an adequate sampling of those exponential functions. Admitting sampling just in the Nyquist limit, the range of distances where the Fresnel patterns are evaluable results:

$$z \geq \frac{\Delta x_0^2}{\lambda N} \tag{8}$$

The same argument can be applied to the global phase factor, multiplying the DFT in expression (6) giving the condition:

$$z \leq \frac{\Delta x_0^2}{\lambda N} \tag{9}$$

A good sampling of the Fresnel pattern is accomplished only if the equality is assumed in both conditions.

Note that, from Eq. (5), if Δx_0 and N are input parameters, for z tending to zero, the output sampling area will tend to zero, and thus, no near-field patterns can be evaluated. As z increases, the output area that is being sampled, i.e. Δx_z wides linearly with the distance, as can be deduced from Eq. (5):

$$\Delta x_z = \frac{\lambda z N}{\Delta x_0} \tag{10}$$

For large values of z, notice that the direct algorithm we just exposed provides the whole extent of the final diffraction pattern. Nevertheless, this result is only compatible with condition (8), coming from appropriate sampling of intensity Fresnel patterns.

As we said in the Introduction, maintaining the number of samples N as a constant leads to methods that provide bad-sampled patterns. Since for long distances the phase has a very rapid variation, this information in the pattern cannot be retrieved because very strong aliasing effects. In a general case, intensity profiles are of soft variation, and thus of easier evaluation than the phase. Because all these reasons the direct-evaluation method is valid for just far-field amplitude evaluation.

An alternative way of evaluating Fresnel diffraction patterns is through the calculation of the propagated angular spectrum [8,9]. The Fourier transform of Eq. (1) can be written as:

$$\tilde{u}_z(\xi) \propto \tilde{u}_0(\xi) \exp(-i\pi\lambda z \xi^2) \tag{11}$$

where the dependence on z of the quadratic phase factor is now just the contrary than in the previous case.

The alternative algorithm will consist of taking the Fourier transform of the input signal, multiplying it by the sampled version of the quadratic phase

factor in Eq. (11), and then performing an inverse Fourier transform, i.e.:

$$(u_z)_\mu \propto \mathrm{DFT}^{-1}\left\{\mathrm{DFT}\left[u_0\left(\frac{m\Delta x_0}{N}\right)\right] \times \exp\left(-i\pi\frac{\lambda z}{\Delta x_0^2}\tilde{m}^2\right)\right\} \quad (12)$$

Now, the Nyquist sampling condition over the quadratic phase factor will provide the following condition:

$$z \leq \frac{\Delta x_0^2}{\lambda N} \quad (13)$$

which holds for both amplitude and phase evaluation, and the method is valid for near-field Fresnel patterns calculation.

There is an apparent contradiction between the two methods explained here. Note that both of them provide an evaluation of the same integral, but they lead to completely different results. The keypoint of all the process is the different use of the DFT algorithm to perform the calculation:

Let us remember that, as we said in the first section, good evaluation of Fresnel patterns requires that the sampling period remains constant for every pattern; i.e. $\delta x_0 = \delta x_z$, independently of the evaluation method. Otherwise, the scaling condition that is imposed by the DFT, when the diffraction pattern is evaluated through Eq. (6) can be derived from Eq. (5):

$$\delta x_z = \frac{\lambda z}{N\delta x_0} \quad (14)$$

and N is an input parameter that will remain constant for every pattern. Thus, we are under the third assumption that was stated in the Introduction, and δx_z must increase with the distance in order that the whole extent of the pattern is sampled.

When angular-spectrum propagation is used instead, the use of two DFT's cancels the scale factor between the input and the output, and finally:

$$\delta x_0 = \delta x_z \quad (15)$$

Thus, the method works under the second assumption (δx_z and N are constants in the propagation process). Since the method is valid for near-distances, we can assume that the algorithm is valid while the size of the pattern does not change significantly.

Note that, in the Nyquist limit, both methods provide the same result. Just by taking the equality in Eqs. (8) and (13), and substituting the result into Eq. (14), we obtain that the sampling there obtained coincides with the one obtained in Eq. (15).

From all this reasoning, we can conclude that every calculation method imposes its own contour conditions over the Fresnel integral that affect the final result. Usually, these contour conditions are imposed at the beginning, and then, a specific algorithm is constructed. In our case, we have followed the inverse way, and thus, an apparent contradiction has appeared.

Summarizing, we have one direct method that allows far-field diffraction patterns calculation, and one method that permits the calculation in the near-field case. Since both methods overlap at a certain distance, the calculation of any distance Fresnel pattern, up to the theoretical limit imposed by the Fresnel integral, is permitted, but not in a single way.

3. Fractional Fourier transform versus Fresnel diffraction integral

The FRT of order $0 < |p| < 2$ of an input function $u_0(x_0)$ provided by a Lohmann Type II system (see Fig. 1) can be expressed as:

$$u_p(x_p) = \exp\left(\frac{i\pi}{\lambda f_1 \tan\phi}x_p^2\right) \times \int_{-\infty}^{\infty} u(x_0)\exp\left(\frac{i\pi}{\lambda f_1\tan\phi}x_0^2\right) \times \exp\left(-\frac{i\pi}{\lambda f_1 \sin\phi}x_0 x_p\right)\mathrm{d}x_0 \quad (16)$$

being $\phi = p\pi/2$, λ the illuminating light wavelength and f_1 an arbitrary fixed length.

Comparing the Fresnel diffraction expression in Eq. (1) and the FRT expression in Eq. (16), one can notice that they are quite similar: both have quadratic phase factors that can not be immediately sampled for all the distances (or p order) range [8]. Nevertheless, calculation of FRT patterns can be done by using one single algorithm for the whole range of p-orders from zero to one, as was shown in Ref. [8] and [13]. Thus, it is interesting to perform a transformation on the Fresnel integral and convert it into a

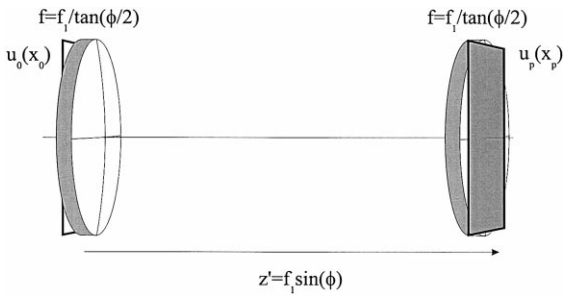

Fig. 1. Lohmann's Type II bulk-optic system for obtaining the FRT pattern of order $p = 2\phi/\pi$ of the input object $u_0(x_0)$.

FRT integral. Doing so, Fresnel calculation algorithms can be reduced to one compact method implying one or two discrete Fourier transforms, which will be applicable in all the range of distances.

In Ref. [17] it is shown, through a formal solution of the wave equation, that the field distribution at any distance from the object can be expressed as an FRT of the input distribution corrected by a scaling function, depending on the distance, and by an additional phase factor. From there, it can be deduced that the final expression for a Fresnel pattern at a distance $z = f_1 \tan\phi$ in terms of an FRT distribution results:

$$u_z\left(\frac{x_p}{\beta}\right) = \exp\left[\frac{i\pi}{\lambda f_1}\frac{x_p^2}{\sin\phi\cos\phi}\right] \times \int_{-\infty}^{\infty} u_0(x_0)\exp\left(\frac{i\pi}{\lambda f_1 \tan\phi}x_0^2\right) \times \exp\left(-\frac{i2\pi}{\lambda f_1 \sin\phi}x_0 x_p\right) \mathrm{d}x_0 = \exp\left(i\pi x_p^2 \frac{\tan\phi}{\lambda f_1}\right) F^p\left[u_0(x_0)\right] \qquad (17)$$

with $\beta = \cos\phi$. Numerical evaluation of the above written expressions needs numerical calculation of an FRT integral and sampling of an additional quadratic phase factor. For the FRT patterns calculation two different methods will be considered here [8,13]. We will call them Single-FFT (S-FFT) and Double-FFT (D-FFT) method, according to the number of FFTs that must be performed to obtain a final FRT distribution.

Note that, aside from other considerations, both methods were based on calculating the FRT integral itself, and sampling the phase factor outside the integral. In the case we are interested in, the amplitude of the scaled Fresnel pattern in Eq. (17) is just the amplitude of the FRT in Eq. (16). Thus, amplitude sampling conditions for the Fresnel case are inherited from the fast-FRT algorithms, and only the phase evaluation will give new sampling conditions.

4. Fresnel diffraction calculation through FRT algorithm

By now, two different algorithms for FRT calculation through the DFT are described in the bibliography [8,13]. The most recent one, that we coined S-FFT, is based on a direct evaluation of the fractional Fourier transform integral. When this algorithm is transformed into a Fresnel calculation method following Eq. (17), it is easy to show that this algorithm is converted into the direct evaluation method we explained in Section 2. Thus, although S-FFT method provides good results when it is applied to the calculation of the FRT integral, it does not provide additional advantages when it is used for Fresnel diffraction calculation.

On the other hand, D-FFT method [8] consists of breaking the FRT integral into different cascaded processes, and not on a direct evaluation of the integral. This particularity will allow us to obtain convenient sampling conditions when the D-FFT algorithm is converted into a Fresnel calculation method.

The D-FFT algorithm is based on Lohmann's Type II configuration, (see Fig. 1). In this method, the different elements affecting the light distribution, i.e. lens, free-space propagation and a second lens, are numerically evaluated and their effect applied to the input distribution. Free space propagation is accomplished, by convenience, in the Fourier domain [8].

The final discrete expression for the FRT obtained through this method is:

$$\left(U_p\right)_\mu = \exp\left[i\frac{-\pi\,\mathrm{sgn}[\sin\phi] + 2\phi + \pi}{4}\right] \times \exp\left[-i\frac{\pi\mu^2}{N}\tan(\phi/2)\right] \times \mathrm{DFT}^{-1}\{\cdots\}$$

$$\{\cdots\} = \left\{ \exp\left[-i\frac{\pi \tilde{m}^2}{N}\sin\phi \right] \times DFT\left\{ u_0\left(\frac{m\Delta x_0}{N} \right) \times \exp\left[-i\frac{\pi m^2}{N}\tan(\phi/2) \right] \right\} \right\} \quad (18)$$

were the relations that have to be fulfilled between input and output sampling areas, coming from the DFT theory are:

$$\Delta x_0 \Delta x_p = \lambda f_1 N \quad (19)$$

where the subindex p refers to the fractional domain. From the free space propagation in the Fourier domain, we obtain [8]:

$$\Delta x_0 = \Delta x_p = \sqrt{\lambda f_1 N} \quad (20)$$

As it was done for the Fresnel calculation algorithms, we will assume that conditions for a fair sampling of expression (18) are obtained from the application of the Nyquist theorem only on the quadratic phase factors affecting the signal. These conditions are:

$$(a)\ |\sin(\phi)| \le 1 \quad (b)\ |\tan(\phi/2)| \le 1 \quad (21)$$

Condition (21a) is always fulfilled, while (21b) will hold only for $\phi \le \pi/2$, or equivalently, $p \le 1$. Anyway, this range covers all domains between object and Fourier domain, and convenient application of the properties of the FRT will permit the extension of the algorithm to any arbitrary range [10].

If we are interested on the calculation of Fresnel patterns, a new condition over the outer phase factor multiplying the fractional Fourier transform in Eq. (17) has to be added to those expressed in Eq. (21), which remain valid for amplitude sampling. Having in mind Eq. (20), and applying the Nyquist theorem over the exponential factor multiplying the FRT in Eq. (17), the new condition that must be fulfilled is:

$$\frac{\Delta x_0^2}{\lambda f_1}\tan\phi \le N \quad \Rightarrow \quad \tan\phi \le 1 \quad (22)$$

which only holds for $\phi \le \pi/4$ or equivalently, since $z = f_1 \tan\phi$, and $z \le f_1$. Therefore the phase of the corresponding Fresnel diffraction pattern cannot be accurately evaluated through the D-FFT method for all distances z, although it can be done for intensity patterns. For the sake of clarity a schematic diagram of the algorithm has been depicted in Fig. 2.

Let us recall that the method described in Eq. (17) will provide a scaled version of a Fresnel distribution. This scaling is inherent to the algorithm. Moreover this ''convenient'' scaling helps to the accuracy of the algorithm, since it impedes the divergence of the field for large z values. The real size of the diffraction pattern obtained through the D-FFT method must be calculated ''a posteriori'', and it results into:

$$\Delta x_z = \frac{\Delta x_p}{\beta} = \frac{\lambda N}{\Delta x_0}\sqrt{z^2 + f_1^2} \quad (23)$$

For short distances z can be neglected in front of f_1. In this case, we can consider than the pattern propagates without changing its size and thus, we are under the same conditions that the spectrum-propagation method: the number of samples N and the

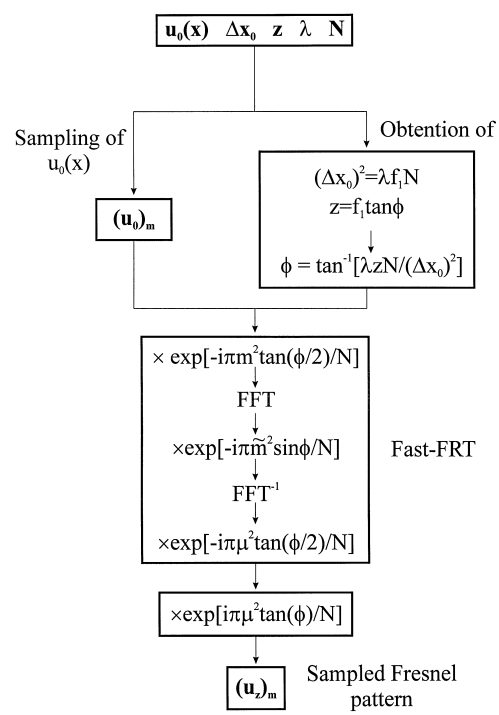

Fig. 2. Schematic representation of the Fresnel-through-FRT algorithm here introduced. The distance z, the wavelength λ and the number of samples N are given as input parameters, together with the optical signal and the input sampling area Δx_0. ϕ can be derived from Eqs. (17) and (20).

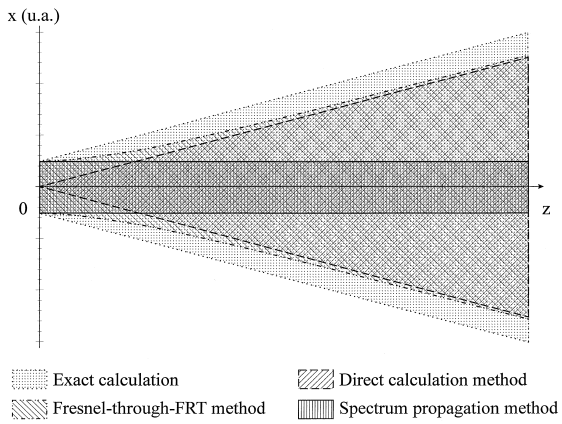

Fig. 3. Extension of the diffracted field obtained through exact calculation, direct method, spectrum propagation method and Fresnel-through-FRT method. The areas hatched inside the lines correspond to each of the methods.

sampling interval δx_z remain constant. Note also, that in this case, both amplitude and phase components of the diffracted field can be calculated.

When z becomes much larger than f_1, the size of the calculated pattern depends linearly with the distance. This is just what happened with the direct evaluation method explained in Section 2 (see Eq. (5)). In this case, N is constant and δx_z increases with the distance, and thus, the global phase factor is not well sampled anymore.

Note that the method just described provides a numerical evaluation of a Fresnel pattern for any distance considered. The results for near and far-field are compatible with the methods obtained in Section 2. What has been gained with the use of the FRT algorithms is the continuity of the z-domain for Fresnel patterns calculation. With the new algorithm, there is no need of splitting the space in two zones, since a continuous transition between object and Fourier domain is obtained.

Summarizing, if one is only interested in obtaining amplitude Fresnel patterns, condition (22) does not apply. In this case, the modulus of the diffraction integral can be evaluated for all the range of distances from object plane to Fourier domain. On the other hand, if we are interested in obtaining the full diffracted pattern, we found some sampling restrictions, imposed by the inherent structure of the diffraction integral. Thus the full Fresnel pattern only can be well sampled in near and medium-field domains. For the far-field case, one have to sacrifice the phase in order to obtain the diffracted pattern in all its extension.

In Fig. 3 we present a schematic representation of the obtained extension of the diffracted field with the methods here presented. As can be appreciated there, the direct method fails when short propagation distances are considered. On the other hand, the spectrum propagation method, is not capable of providing a complete view of the diffracted field when dealing with long distances. Finally, note that the Fresnel-through-FRT method allows a complete reproduction of the diffracted field at any distance, provided that only amplitude is considered.

5. Computer simulations

Some computer simulations have been presented to test the performance of the algorithms here introduced. In Fig. 4 we represent several diffraction

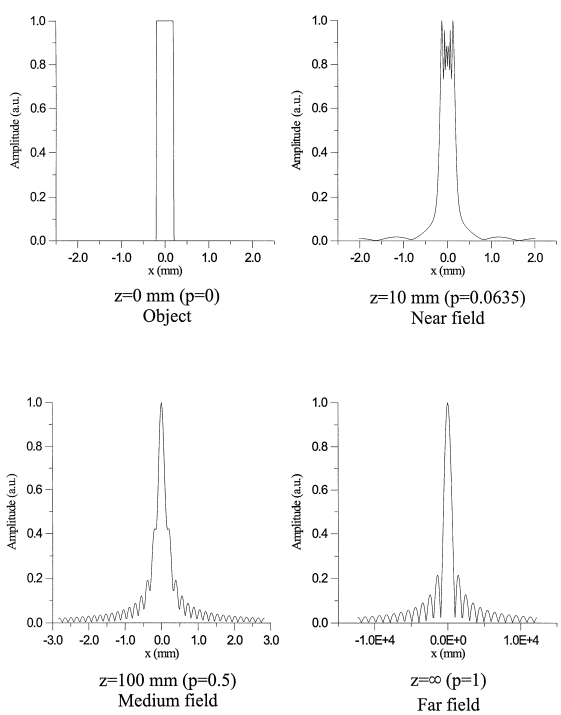

Fig. 4. Object and exact Fresnel diffraction patterns of a rectangle with width $a = 0.4$ mm calculated through Eq. (17). The patterns correspond to the object itself, near, medium and far-field. p values are provided only for later comparisons.

patterns (near, medium and far-field) corresponding to a rectangle of width 0.4 mm. The patterns have been exactly calculated through mathematica. Only the amplitude is represented, since the phase distribution does not add any relevant visual information. The patterns in Fig. 4 will serve as a reference for checking the accuracy of the numerical methods described along the paper.

In Figs. 5–7 the distributions obtained with the algorithms here discussed are depicted. For every distance we have plot the amplitude distribution. The comparison between exact and calculated field for every sample is also provided. These diagrams are calculated for amplitude and phase distribution. In some of them we have marked some relevant samples that will be analyzed in what follows.

In Fig. 5 we have presented the obtained results for the direct calculation method. Note that, as it was explained before, this algorithm only reproduces a small area of the diffraction pattern when short distances are considered (see Fig. 3). Regarding the accuracy of the obtained results, note that the amplitude is well evaluated for medium and large distances, while for the phase this occurs for short and medium values of z. These results agree with Eqs. (8) and (9) which established the conditions for a well sampled pattern. For the cases not fulfilling these conditions (near-field amplitude and far-field phase distributions), the aliasing effect is the responsible of the calculation error. If we point our attention on the central samples of the calculated pattern (these points are marked in the diagrams), we can see that the direct calculation algorithm is capable of reproducing the theoretical results in amplitude and phase for all the considered distances. Summarizing, the direct calculation algorithm allows the calculation of near, medium and far-field diffraction pattern but affected with aliasing effects. Nevertheless, the sampling area near the object goes to zero (see Fig. 3), and thus the method is not operative for complete diffraction fields calculations.

Regarding the diffraction patterns calculation algorithm through spectrum propagation, (see Fig. 6) let us remember that the method is valid if condition (13) is fulfilled. Thus, far field patterns will not be accurately sampled. Furthermore, this algorithm provides, for all distances, the same extension of the output area. Hence, the Fourier distribution provided by it will only reproduce a small central area of the total pattern. In the case we are considering here, this area corresponds to the central lobe of a *sinc* function, which does not go to zero at the border of the sampling window, and thus, aliasing effects will destroy completely the signal [1], as can be seen in Fig. 6. For near and medium field patterns, the method reproduces, more or less accurately the amplitude and phase of the considered distribution. It is worth noting that, although Eq. (13) is fulfilled, we can easily appreciate some reconstruction errors in the amplitude distribution for the near field case. These errors become more evident when phase distributions are considered. The problem does not appear because an aliasing effect but a vignetting effect and it is caused by an inappropriate evaluation of the quadratic phase factors. Since short distances imply a very soft variation of the quadratic phase factor in Eq. (12), the fast oscillations go out of the sampling area, and the effective factor acts no more like a quadratic phase exponential. As z enlarges, the effect becomes less noticeable, although it does exist for any distance, provided that the evaluation window is always of finite extension. It is worth noting that in any case, phase distributions are much more sensible to this cut-off effect that amplitude distributions. Since the last ones usually present low values at the borders of the window, the final effect will not be important, in terms of absolute error. On the other hand, in the border of the window, the phase tends to

Fig. 5. Fresnel diffraction patterns of a rectangle with width $a = 0.4$ mm calculated through the direct method. Calculated amplitude fields and comparative results with the exact field. p values are provided only for later comparisons.

Fig. 6. Fresnel diffraction patterns of a rectangle with width $a = 0.4$ mm calculated through the spectrum propagation method. Calculated amplitude fields and comparative results with the exact field. p values are provided only for later comparisons.

Fig. 7. Fresnel diffraction patterns of a rectangle with width $a = 0.4$ mm calculated through the fast FRT algorithm. Calculated amplitude fields and comparative results with the exact field.

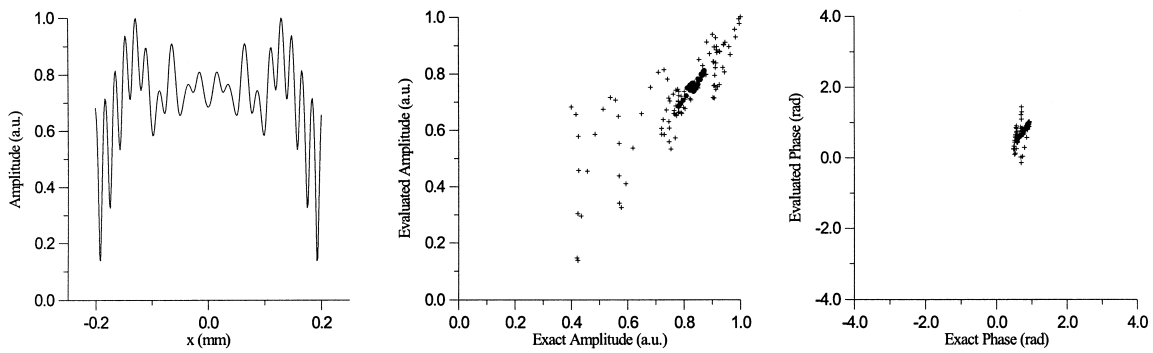

z=10 mm (p=0.0635)
Near field

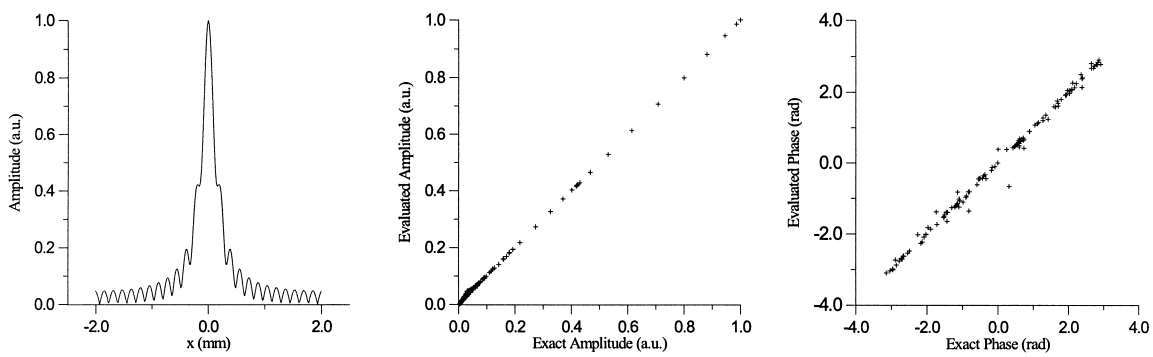

z=100 mm (p=0.5)
Medium field

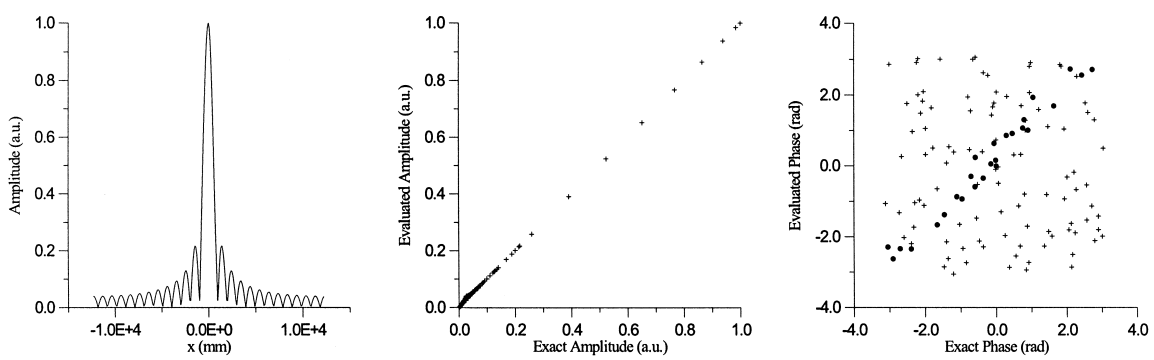

z=∞ (p=1)
Far field

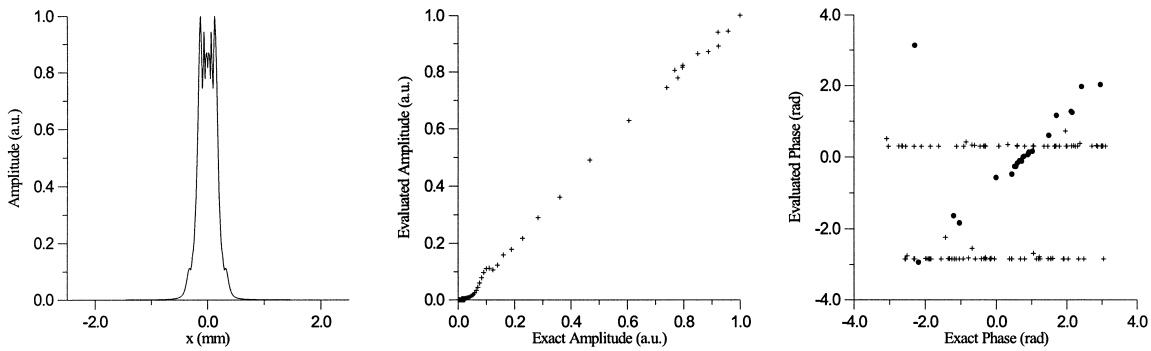

z=10 mm (p=0.0635)
Near field

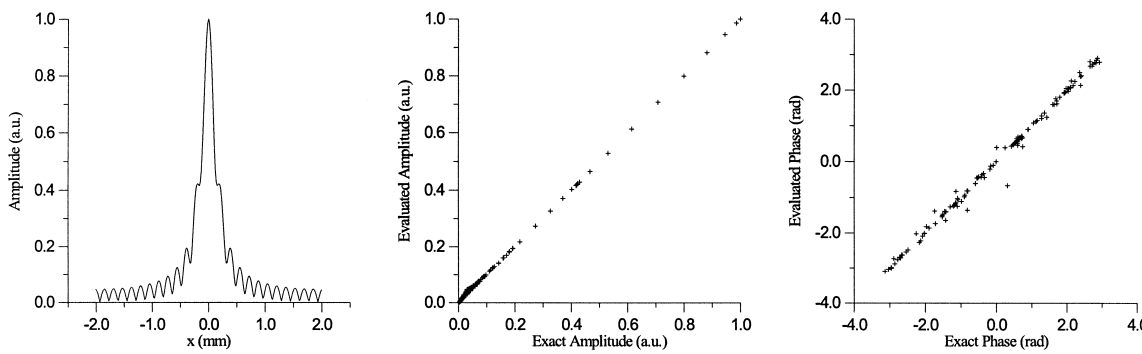

z=100 mm (p=0.5)
Medium field

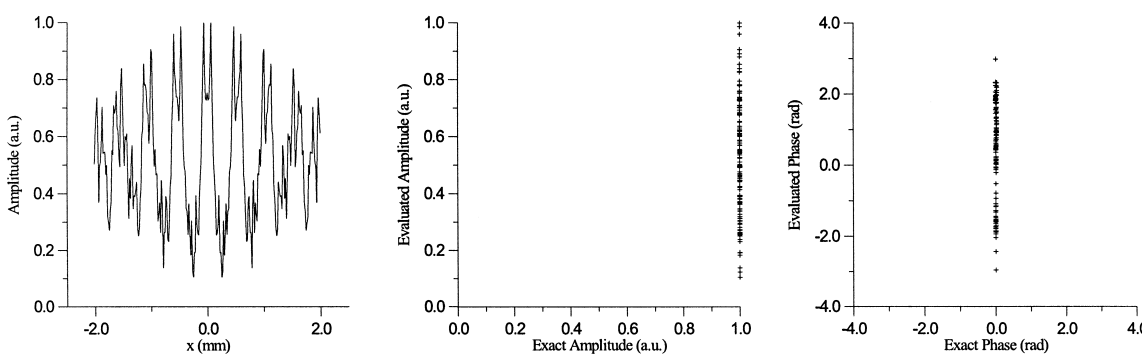

z=∞ (p=1)
Far field

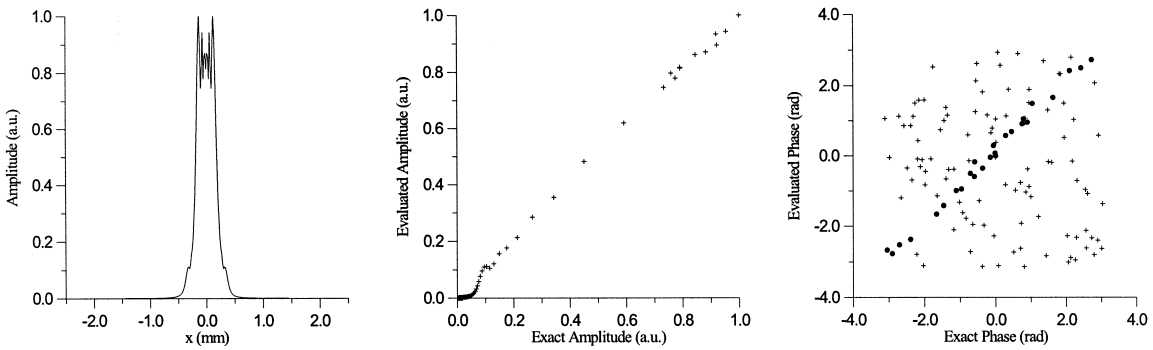

z=10 mm (p=0.0635)
Near field

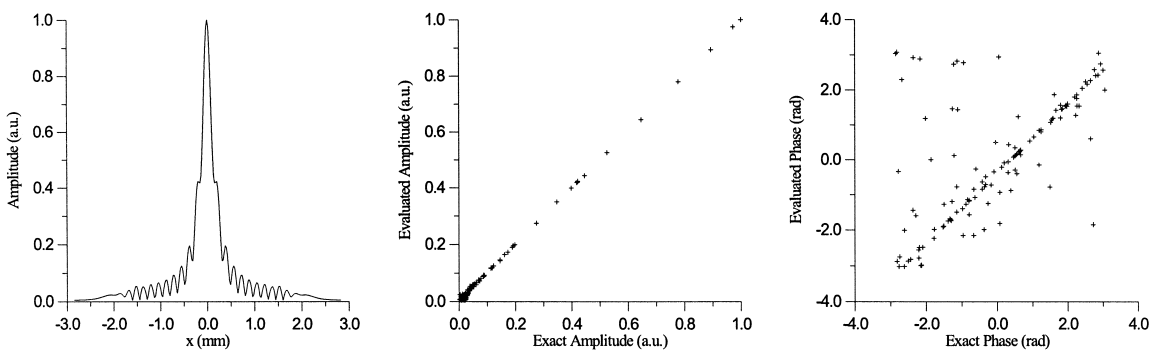

z=100 mm (p=0.5)
Medium field

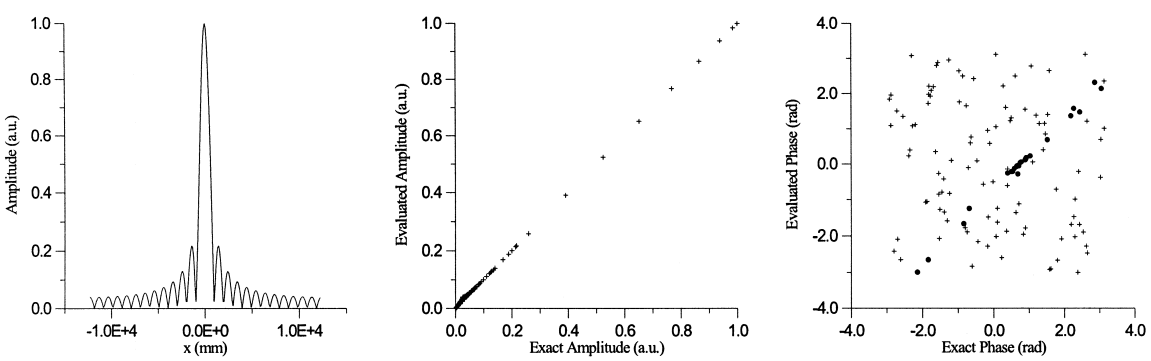

z=∞ (p=1)
Far field

oscillate very fast, and thus, any sampling error in this part,will contribute dramatically to increment the calculation error.

In Fig. 7, we plot the results obtained through the algorithm we have introduced. Note that, with this algorithm, the sampling area wides conveniently with the distance as it is depicted in Fig. 3. Regarding the performance of this method, let us recall that there are not restrictions about the sampling rate of amplitude distributions (21), but there are for the phase components (22). This assertion agrees with the obtained results. For amplitude distributions we obtain an accurate reproduction of the theoretical result and only the near field pattern is affected by the vignetting effect we explained previously. Concerning the phase results, one can see that the vignetting effect affects the near-field distribution, although the central points are correctly evaluated. For far-field distributions, condition (22) is not fulfilled, and thus, aliasing effects will distort the final result.

As an application of the algorithm here introduced, we present in Fig. 8 the diffraction field obtained for a double aperture. Each row of the figure represents a different diffraction pattern. The whole field consists of 256 diffraction patterns of a vector of $N = 256$ samples. We can easily see how the interferences appear as the field propagates, and the typical interference fringes at the Fourier plane. Note that this plot needs $O(N \log N)$ operations, while the exact calculation will need $O(N^2)$ operations, and thus, much more computation time. Note also that this kind of plots can only be done with the Fresnel-through-FRT algorithm, since the other methods here described present serious problems of aliasing and inadequate sampling areas for amplitude calculations.

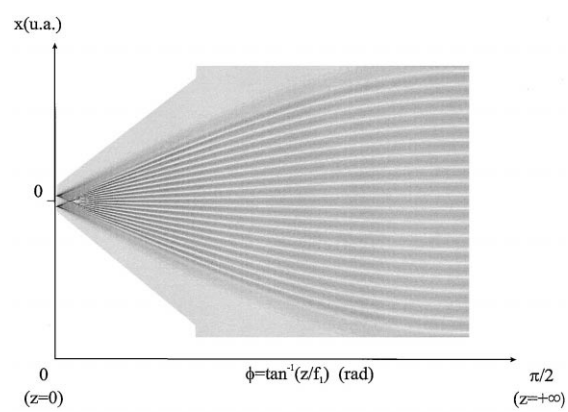

Fig. 8. Example of application of the algorithm here introduced. Diffraction field of a double slit, plotted from $z = 0$ to $z = \infty$.

6. Conclusions

Some topics regarding the numerical calculation of the Fresnel integral have been discussed here. The special form of this integral does not lead to easy sampling conditions. It is demonstrated here that, independently of the evaluation method, it is not possible to obtain a well sampled Fresnel pattern in its whole spatial extent for every distance, and thus, in most cases a compromise result has to be applied.

Some fast algorithms using the FFT for diffraction patterns calculation have been analysed here, and their performance has been checked. These methods are of easy implementation, but are only valid for a specific range of distances: near-field or far-field. Nevertheless, those methods are compatible when medium distances are considered, permitting the calculation of the Fresnel integral in all the range of distances, but not in a single way.

Fast algorithms for FRT calculation allow the evaluation of this integral from object to Fourier domain in a single step, providing accurate results. The resemblances between the FRT integral and the Fresnel integral have been exploited here to design a fast Fresnel through FRT algorithm. The obtained algorithm results are accurate and of easy implementation. Although the calculated patterns are affected by aliasing and vignetting effects, the method provides very good results in reproducing amplitude patterns. Some numerical simulations demonstrate the feasibility of the algorithm here introduced.

Acknowledgements

This work has been partially financed by the Spanish DGCYT project number PB96-1134-C02-02. L.M. Bernardo acknowledges the financial support granted by PRAXIS XXI and FEDER under the project PRAXIS/2/2.1/FIS/55/94.

References

[1] R.C. Gonzalez, P. Witz, Digital Image Processing, Addison Wesley Pub. Company, MA, 1987.
[2] J.W. Cooley, J.W. Tukey, Math. Comput. 19 (1965) 297.
[3] J.W. Goodman, Introduction to Fourier Optics, McGraw-Hill, New York, 1968.
[4] R. Barakat The calculation of integrals Encountered in Optical Diffraction Theory, B.R. Frieden (Ed.), in: Topics in Applied Physics 41, Springer-Verlag Berlin, 1980.
[5] W.H. Southwell, J. Opt. Soc. Am. A 1 (1981) 7.
[6] L.A. D'Arcio, J.M. Braat, H.J. Frankena, J. Opt. Soc. Am. A 11 (1994) 2664.
[7] E. Carcole, S. Bosch, J. Campos, J. Mod. Opt. 40 (1993) 1091.
[8] J. Garcia, D. Mas, R.G. Dorsch, Appl. Opt. 35 (1996) 7013.
[9] D. Mendlovic, Z. Zalevsky, N. Konforti, J. Mod. Opt. 44 (1997) 407.
[10] D. Mendlovic, H.M. Ozaktas, J. Opt. Soc. Am. A 10 (1993) 1875.
[11] H.M. Ozaktas, D. Mendlovic, J. Opt. Soc. Am. A 10 (1993) 2522.
[12] A.W. Lohmann, J. Opt. Soc. Am. A 10 (1993) 2181.
[13] F.J. Marinho, L.M. Bernardo, J. Opt. Soc. Am. A. 15 (1998) 2111.
[14] P. Pellat-Finet, Opt. Lett. 19 (1994) 1388.
[15] D. Dragoman, M. Dragoman, Opt. Commun. 141 (1997) 5.
[16] J. Shamir, N. Cohen, J. Opt. Soc. Am. A 12 (1995) 2415.
[17] T. Alieva, V. Lopez, F. Agullo-Lopez, L.B. Almeida, J. Mod. Opt. 41 (1994) 1037.
[18] J. Garcia, R.G. Dorsch, A.W. Lohmann, C. Ferreira, Z. Zalevsky, Opt. Commun. 133 (1997) 393.
[19] L.M. Bernardo, O.D.D. Soares, Opt. Commun. 110 (1994) 517.